

Directive emission from high- Q photonic crystal cavities through band folding

Nguyen-Vi-Quynh Tran, Sylvain Combrié, and Alfredo De Rossi*

Thales Research and Technology, Route Départementale 128, 91767 Palaiseau, France

(Received 24 October 2008; revised manuscript received 3 December 2008; published 6 January 2009)

We propose a design methodology for high- Q photonic crystal nanocavities with a tailored radiation pattern. As an example, we applied this technique to five missing hole defect cavities and experimentally achieved a sixfold improvement of the collection efficiency. This will enable high external efficiency in single-photon sources based on photonic crystal nanocavities.

DOI: [10.1103/PhysRevB.79.041101](https://doi.org/10.1103/PhysRevB.79.041101)

PACS number(s): 42.70.Qs, 42.60.Da, 42.55.Tv, 41.20.Jb

The first experimental demonstration of high quality factors achieved in two-dimensional (2D) nanocavities is connected to the deep understanding of the way radiation leaks out of photonic crystals (PCs).¹⁻³ Ultra-high- Q (10^6) single-mode microcavities have been demonstrated based on Si membrane PCs (Refs. 4 and 5) and on III-V semiconductors.⁶ Two-dimensional PCs are known to provide effective-field confinement [the modal volume is on the order of $(\lambda/n)^3$ or even smaller] along with a large Q factor, thus providing extremely high values for the Purcell factor.¹ By enhancing the spontaneous emission rate and thereby the efficiency of point sources embedded in high index materials, this makes them suitable candidates in particular for cavity quantum electrodynamics and single-photon sources.⁷⁻⁹

However, in contrast with micropillars, originally proposed as optical microcavities,¹⁰ the directivity of the radiation emitted from PC microcavities is poor and this limits the coupling efficiency of the emitted photons to the output channel severely. Therefore, the advantage of achieving the highest Q/V ratio cannot be exploited entirely without an improvement of directivity.

More generally, coupling light efficiently in and out of photonic crystals is crucial and it is very difficult because of the large mode mismatch between highly confined photonic modes inside these structures and modes in the free space or in optical fibers. Photonic crystal cavities have been proposed as an elegant way to couple radiation into PC structures.^{11,12} An unprecedented control over the beaming from a single mode diode laser has been demonstrated, however, this was based on a spatially extended band-edge mode.¹³

Controlling the radiation emitted from a PC membrane nanocavity is harder for two fundamental reasons: first, the extremely reduced modal volume implies a very strong diffraction; the second reason is intimately related to the optimization procedure of high- Q cavities. The starting point of this procedure is the relation between the near field of the mode represented in the reciprocal space and its far field. Leakage is minimized by reducing the field inside the light circle (i.e., $|\vec{k}| < \omega/c$).¹⁻³ This implies that the far field is determined by the residual near field inside the light circle and, for this reason, it is difficult to control. Kim and co-workers¹⁴ have shown theoretically that a suitable optimization of a particular kind of cavity (hexapole) allows the reshaping of the far field into an almost Gaussian mode and that the collection efficiency can be increased to 80%. The

optimization procedure, specific to this cavity, is focused on the modification of two holes. This makes far field particularly sensitive to disorder.

In this Rapid Communication we introduce a design procedure which applies to a variety of small-volume high- Q cavities and which is very robust to disorder. As an example, we have developed a modified $L5$ cavity and experimentally demonstrated a strong increase in the extraction efficiency compared to a standard microcavity. The main idea is illustrated in Figs. 1(a) and 1(b). The near field of an optimized PC cavity is distributed as close as possible to the border of the Brillouin zone (BZ), which is at $k_x = \pi/a$. If a period $2a$ is superimposed to the original structure, the distribution of

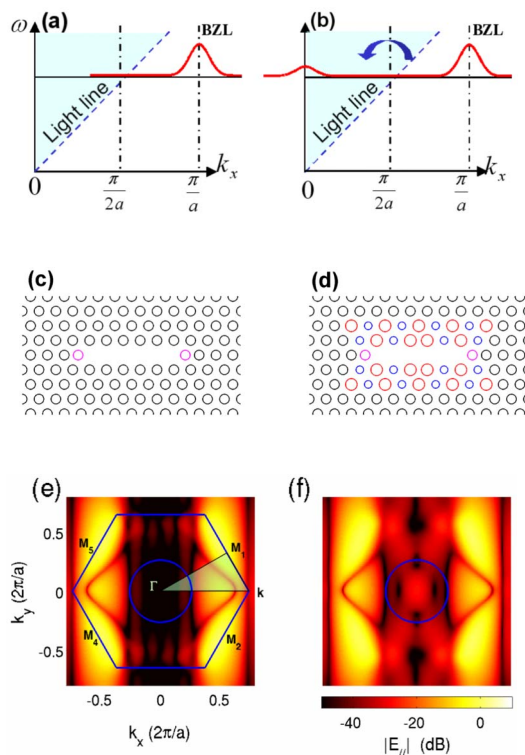


FIG. 1. (Color online) Principle of band folding: (a) schematic representation of the near field distribution in the reciprocal space for an optimized cavity; (b) band-folded distribution. Designs implementing the principle on 2D membrane cavities: (c) $L5$ cavity, (d) modified $L5$ (emphasized). [(e) and (f)] Calculated distributions (pseudocolor map) of the near field corresponding to (c) and (d). First BZ, reduced BZ, and light circle are represented.

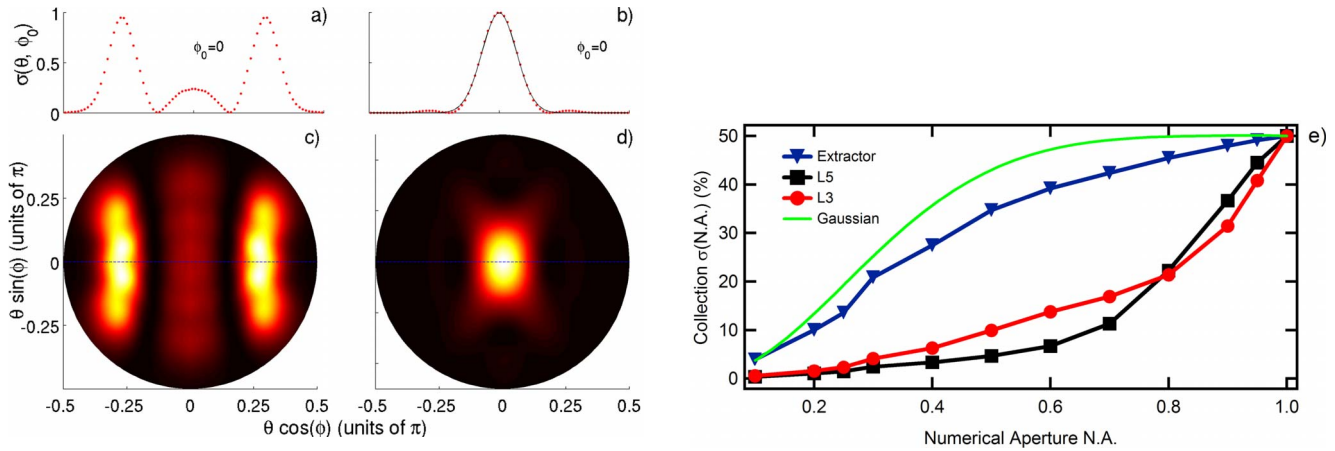


FIG. 2. (Color online) Calculated radiation $P(\theta, \phi)$ using Eq. (1), corresponding to the $L5$ cavity [Fig. 1(c)] and the extractor [Fig. 1(d)]. Panels (a) and (b) plot $P(\theta, \phi=0)$ corresponding to the $L5$ and the extractor cavity. A Gaussian fit is added. Panels (c) and (d) map $P(\theta, \phi)$ on $x = \theta \cos(\phi)$ and $y = \theta \sin(\phi)$. Panel (e) shows the fraction of $P(\theta, \phi)$ which would be collected as a function of the numerical aperture of the optics. The calculation is also reported for a $L3$ cavity. The ideal curve for a Gaussian beam with $\theta_x = 0.13\pi$ and $\theta_y = 0.2\pi$.

the near field in the reciprocal space is folded with respect to $k_x = \pi/(2a)$ and therefore a replica of the distribution near the first BZ appears at $k_x = 0$. Consequently, radiation is now leaked mainly vertically and the amount of leakage is controlled by the amplitude of the subharmonics with period $2a$. This concept has been discussed theoretically in the field of plasmonics.¹⁵ The analogy with grating coupling to waveguides is convenient to understand band folding and has been adapted to PC waveguides (not cavities) for a very different purpose, i.e., imaging.¹⁶ A nice feature of band folding is that if the near field distribution corresponding to the original structure is bell shaped, so will be its replica at $k_x = 0$ and the radiation pattern. To illustrate this principle we designed an optimized $L5$ cavity [Fig. 1(c)] with a resonant mode at 1575 nm and a high intrinsic Q factor (about 250 000). The design parameters are the following: lattice period $a = 415$ nm, slab thickness $h = 265$ nm, normalized radius $r = 0.29a$ and normalized shift of the two side holes, $s = 0.18a$. Calculations have been performed with the three-dimensional (3D) finite differences in time domain method running on a computer cluster. The resolution of the finite differences grid is $\Delta x = a/16$ and accuracy was improved using the technique in Ref. 17. The relative accuracy on the resonant frequency f_0 was 0.2% after the convergence test. The $L5$ cavity was then modified [Fig. 1(d)] in order to implement the band-folding concept. We refer to this structure as the *extractor*. The diameter of the holes was changed periodically [Fig. 1(d)] in order to introduce new lattice vectors which fold the M points into Γ . The value used in this work is $|\Delta r/r| = 0.01$. This is apparent in Figs. 1(e) and 1(f), where the electric field parallel to the slab surface ($|\tilde{E}_{\parallel}|^2$) is represented in the reciprocal space (i.e., the spatial Fourier transform). An approximation suitable for planar structures^{3,14,18} relates the electric and magnetic fields parallel to the surface to the radiation pattern $\sigma(\theta, \phi)$ through

$$\sigma \approx A \int \int_{|\tilde{k}_{\parallel}| < \omega/c} |\tilde{H}_y + \tilde{E}_x/\eta_0|^2 + |\tilde{H}_x - \tilde{E}_y/\eta_0|^2 dk_{\parallel}^2. \quad (1)$$

Here $A = \omega^2/(8\pi\eta_0 c^2)$ and $\sigma(\theta, \phi)$ is defined as the normalized radiated power, i.e., $\sigma(\theta, \phi) = P(\theta, \phi)/(W\omega_0)$ with

$P(\theta, \phi)$ the power, W the energy in the mode, and η_0 is the vacuum impedance. Importantly, as the relevant mode in dielectric 2D PCs is quasi-TE, the dominant contribution is from the electric field.³

Figure 1(e) shows that the design of the $L5$ cavity [Fig. 1(c)] minimizes the field within the light circle ($|\tilde{k}_{\parallel}| < \omega/c$) and thereby the radiated power. The near field is mainly distributed around the M_1, M_2, M_4, M_5 points in the reciprocal space. In contrast, the design in Fig. 1(d) produces a replica of the four peaks ($M_1, 2, 4, 5$) at the Γ point in Fig. 1(f); thus we succeeded in reshaping the near field in the light circle. The Q factor of the extractor is $Q_{ex} = 3.9 \times 10^4$ and it is lower than that of the original structure ($Q_0 = 2.5 \times 10^5$). The fraction of radiation which is funneled into the bell-shaped mode centered in $k=0$ is approximately $1 - Q_{ex}/Q_0 \approx 85\%$. Thus, the larger the Q factor of the original cavity, the larger the potential extraction efficiency or the Q factor allowed for the extractor.

The effectiveness of the design in controlling the far-field emission is proven by direct calculation using formula (1) and shown in Fig. 2. While the radiation pattern of the $L5$ cavity is rather complicated [Figs. 2(a) and 2(c)] and mainly distributed at large azimuthal angles θ , the pattern associated to the modified $L5$ cavity (the extractor) is a bell-shaped pattern [Figs. 2(b) and 2(d)] and centered at $\theta=0$, i.e., the vertical direction.¹⁹

After fitting with an elliptical Gaussian beam we obtain the values for the aperture (half-width at $1/e^2$) to be $\theta_x = 0.13\pi$ (NA=0.4) and $\theta_y = 0.2\pi$ (NA=0.6), with $\phi=0$ and $\phi=\pi/2$, respectively. The normalized collection efficiency, i.e., the amount of radiation which can be collected with an optics with numerical aperture NA is $\sigma(\text{NA}) = \int_{2\pi}^{\text{arcsin}(\text{NA})} \sigma(\theta, \phi) d\theta d\phi$. This is plotted in Fig. 2(e). Because of the symmetry of the PC slab, the maximum theoretical collection is 50% (theoretical curve is plot for an ideal Gaussian beam). This figure can be improved by exploiting the reflection from the substrate, as suggested in Ref. 14. We have not considered this possibility in our calculations and we calculated the amount of energy collected from one side of the membrane only.

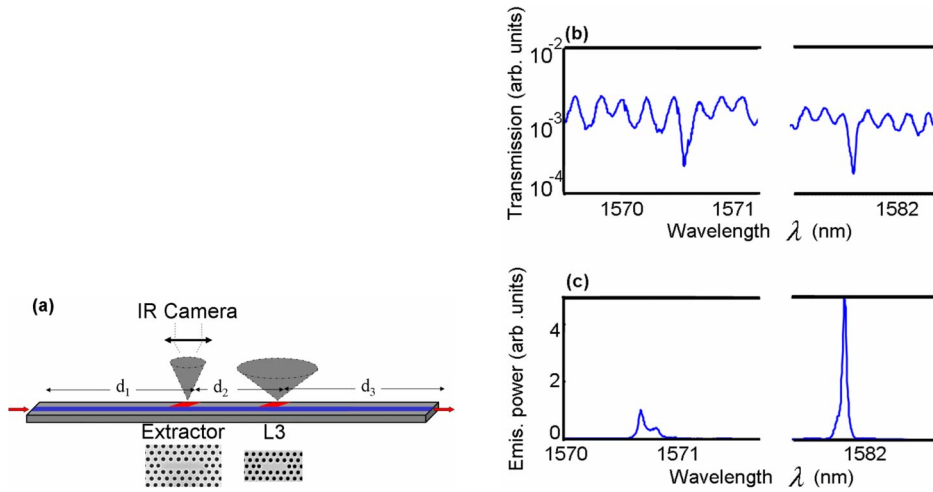


FIG. 3. (Color online) (a) Schematic description of the sample and SEM image of the cavities ($d_1=500 \mu\text{m}$, $d_2=200 \mu\text{m}$, $d_3=300 \mu\text{m}$); (b) transmission and (c) off-plane emission from the $L3$ (reference) cavity (1571 nm) and the extractor (1582 nm).

In Fig. 2(e) it is apparent that the collection efficiency of the extractor is far better (sixfold improvement with $\text{NA}=0.25$) than that of the $L5$ and an $L3$ cavity.¹ In fact, optics with $\text{NA}>0.9$ are required in order to collect at least 30% of the radiation emitted from the surface of the $L3$ or $L5$ cavities, while the extractor only requires $\text{NA}=0.4$ for the same efficiency. In addition, 45% is achieved with $\text{NA}=0.8$, which is the kind of optics used in setups for low temperature spectroscopy.

We have validated this design experimentally in the following way. The sample structure is shown in Fig. 3(a) (scanning electron microscope [SEM] figure is also shown). The sample is a GaAs slab (thickness is 265 nm) patterned with a triangular lattice (period $a=415 \text{ nm}$) of holes with radius $r=0.29a$. The fabrication process and the detailed linear characterization of similar structures are described elsewhere.^{20,21} Two PC cavities are side coupled to the same PC waveguide (width $W=1.05\sqrt{3}a$). One, the reference cavity, is the optimized $L3$ cavity;¹ the holes at the cavity edge were shifted by $s=0.15a$. The other is the extractor, with parameters corresponding to the calculations in Figs. 1 and 2. The spacing between the two cavities and the waveguide is four and five rows, respectively.

We measure the waveguide transmission spectra Fig. 3(b) and the off-plane radiation Fig. 3(c) collected from each of the two cavities with a microscope objective ($\text{NA}=0.4$ here) and an InGaAs infrared camera (Xenics). A narrow linewidth ($\ll 1 \text{ MHz}$) tunable laser (Santec TSL 520c) was used. Figure 3(c) shows that the off-plane emission P_e from the modified $L5$ cavity (at $\lambda=1581 \text{ nm}$) is about five times stronger than the reference (at $\lambda=1571 \text{ nm}$). Accurate comparison of the directivity of the two cavities must take into account the actual value of the drop efficiencies (i.e., the ratio between the power leaking from the cavity and that which is coupled into the waveguide). The drop efficiency at resonance is estimated through $\epsilon=1-T-R=2Q^2/(Q_0Q_c)$, with T and R being the transmission and the reflection of the waveguide,²² Q_0 is the isolated cavity Q factor, i.e., for vanishing coupling ($Q_c=\infty$). We measured $Q=24\,000$ and $Q=25\,000$ for the reference and the modified $L5$ cavity, respectively. Using the relation $Q_0=Q\sqrt{T}/T_{\text{res}}$ we get, from the transmission [Fig. 3(b)], the estimated intrinsic Q factors ($Q_0^{L3}=45\,000$ and

$Q_0^{L5}=58\,000$). Here T and T_{res} are the transmission out of the cavity resonance and at resonance, respectively. The calibrated ratio of the collection efficiencies is then $\sigma_{L5}/\sigma_{L3}=P_e^{L5}/P_e^{L3}(\epsilon^{L3}/\epsilon^{L5})=4$ which is in good agreement with theory.

In order to provide a strong experimental evidence that the modified $L5$ cavity reshapes the radiated far field and provides a bell-shaped beam perpendicular to the surface of the cavity, we have repeated this measurement by varying the numerical aperture of the microscope objective from 0.25 to 0.95. Direct far-field measurement (i.e., without microscope objective) is difficult because of strong scattering from the waveguide input facet. In contrast, in our experimental configuration the input facet is well outside the image field (with size $<200 \mu\text{m}$, while cavity to facet distance is $500 \mu\text{m}$) and no stray light is detected by the camera. The measurement is calibrated with the transmission of each microscope objective. The result of the measurement is shown in Fig. 4(a) and it is compared with the theoretical result calculated by the 3D FDTD method. The agreement is excellent on all the measured points. The comparison in terms of collection efficiency in Fig. 4(b) shows that the collection efficiency of the extractor cavity is much stronger compared to $L3$ and $L5$ cavities when the numerical aperture is small. This implies that the cavity emits on a beam with reduced divergence. We have obtained similar results with other pairs of reference or modified $L5$ cavities (16 in total), thus confirming the expected robustness with respect to structural disorder. We also found that the beam emitted from the cavity is linearly polarized on the PC plane, perpendicular to the long axis of the cavity, as expected from modeling.

We have introduced a concept for designing high- Q photonic crystal nanocavities with a well controlled far-field pattern. This allows vertical emitting devices with very good emission efficiency, on the order of 80% if a mirror is used. This is a potential breakthrough for suitable single-photon sources for quantum optics based on PCs. The design strategy proposed here does not result from “trial and error” optimization; instead, it exploits the fundamental properties of photonic crystals. We believe that this result will solve the crucial issue of improving the collection efficiency from

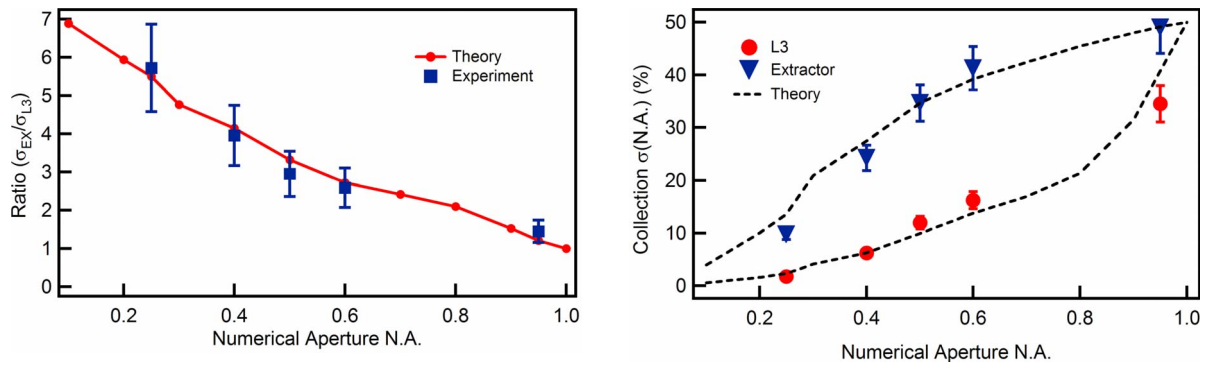


FIG. 4. (Color online) (a) Measured and theoretical ratio of the collection efficiency for the extractor and the reference (L3) as a function of the numerical aperture of the collection optics. (b) Collected power, measured. Theory from Fig. 2(c) is superimposed (dashed line).

single-photon sources based on photonic crystals. Although we modulated the hole diameter in order to achieve band folding, the same result can also be achieved through other kinds of perturbation of the PC lattice (e.g., hole displacement).

This work was partly funded by the European Commission within the project QPhoton under Contract No. IST-029283. Authors would like to thank G. Cassabois (ENS Paris) for valuable discussions and Simone Cassette for support in device processing.

*alfredo.derossi@thalesgroup.com

¹Y. Akahane, T. Asano, B. Song, and S. Noda, *Nature (London)* **425**, 944 (2003).

²K. Srinivasan and O. Painter, *Opt. Express* **10**, 670 (2002).

³J. J. Vučković, M. Lončar, H. Mabuchi, and A. Scherer, *IEEE J. Quantum Electron.* **38**, 850 (2002).

⁴B. S. Song, S. Noda, T. Asano, and Y. Akahane, *Nature Mater.* **4**, 207 (2005).

⁵E. Kuramochi, M. Notomi, S. Mitsugi, A. Shinya, and T. Tanabe, *Appl. Phys. Lett.* **88**, 041112 (2006).

⁶S. Combrié, A. De Rossi, Q. N. V. Tran, and H. Benisty, *Opt. Lett.* **33**, 1908 (2008).

⁷A. Badolato, K. Hennessy, M. Atature, J. Dreiser, E. Hu, P. M. Petroff, and A. Imamoglu, *Science* **308**, 1158 (2005).

⁸W.-H. Chang, W.-Y. Chen, H.-S. Chang, T.-P. Hsieh, J.-I. Chyi, and T.-M. Hsu, *Phys. Rev. Lett.* **96**, 117401 (2006).

⁹W. C. Stumpf, M. Fujita, M. Yamaguchi, T. Asano, and S. Noda, *Appl. Phys. Lett.* **90**, 231101 (2007).

¹⁰J. M. Gérard, B. Sermage, B. Gayral, B. Legrand, E. Costard, and V. Thierry-Mieg, *Phys. Rev. Lett.* **81**, 1110 (1998).

¹¹S. Noda, A. Chutinan, and M. Imada, *Nature (London)* **407**, 608 (2000).

¹²M. Imada, S. Noda, A. Chutinan, M. Mochizuki, and T. Tanaka,

J. Lightwave Technol. **20**, 873 (2002).

¹³E. Miyai, K. Sakai, T. Okano, W. Kunishi, D. Ohnishi, and S. Noda, *Nature (London)* **441**, 946 (2006).

¹⁴S.-H. Kim, S.-K. Kim, and Y.-H. Lee, *Phys. Rev. B* **73**, 235117 (2006).

¹⁵M. Carras and A. D. Rossi, *Opt. Lett.* **31**, 47 (2006).

¹⁶N. LeThomas, R. Houdré, L. H. Frandsen, J. Fage-Pedersen, A. V. Lavrinenko, and P. I. Borel, *Phys. Rev. B* **76**, 035103 (2007).

¹⁷A. Farjadpour, D. Roundy, A. Rodriguez, M. Ibanescu, P. Bermel, J. D. Joannopoulos, S. G. Johnson, and G. W. Burr, *Opt. Lett.* **31**, 2972 (2006).

¹⁸L. Stabellini, M. Carras, A. De Rossi, and G. Bellanca, *IEEE J. Quantum Electron.* **44**, 905 (2008).

¹⁹See EPAPS Document No. E-PRBMDO-78-R12848 for more details on fitting to a Gaussian beam. For more information on EPAPS, see <http://www.aip.org/pubservs/epaps.html>.

²⁰S. Combrié, S. Bansropun, M. Lecomte, O. Parillaud, S. Cassette, H. Benisty, and J. Nagle, *J. Vac. Sci. Technol. B* **23**, 1521 (2005).

²¹S. Combrié, E. Weidner, A. De Rossi, S. Bansropun, S. Cassette, A. Talneau, and H. Benisty, *Opt. Express* **14**, 7353 (2006).

²²Y. Xu, Y. Li, R. K. Lee, and A. Yariv, *Phys. Rev. E* **62**, 7389 (2000).